



Phylogeny of Mesitiinae (Hymenoptera: Bethyridae): assessing their classification, character evolution and diversification

Diego N. Barbosa¹, Marcel Gustavo Hermes², Anderson Lepeco³

¹ Universidade Federal do Paraná, Campus III – Centro Politécnico, Av. Coronel Francisco Heráclito dos Santos, s/n, Jardim das Américas, 81.531-980, Curitiba, PR, Brazil

² Universidade Federal de Lavras, Campus Universitário, Departamento de Biologia, Av. Central s/n, 37.200-900, Lavras, MG, Brazil

³ Laboratório de Biologia Comparada e Abelhas, Departamento de Biologia, Faculdade de Filosofia, Ciências e Letras de Ribeirão Preto, Universidade de São Paulo, Avenida Bandeirantes, 3900. 14040-901, Ribeirão Preto, SP, Brazil

<http://zoobank.org/5B8D112E-AAC7-4F2E-AC98-A057F6094793>

Corresponding author: Diego Nunes Barbosa (barbosa.laelius@gmail.com)

Received 17 May 2022

Accepted 03 November 2022

Published 22 November 2022

Academic Editors Ângelo Pinto, Mónica M. Solórzano-Kraemer

Citation: Barbosa DN, Hermes MG, Lepeco A (2022) Phylogeny of Mesitiinae (Hymenoptera: Bethyridae): assessing their classification, character evolution and diversification. *Arthropod Systematics & Phylogeny* 80: 603–625. <https://doi.org/10.3897/asp.80.e86666>

Abstract

We present the first phylogenetic hypothesis for Mesitiinae based on 112 morpho-structural characters and 61 species. The results did not support Argaman's tribal classification for Mesitiinae, since no tribes were found to be monophyletic. *Anaylax* was found to be paraphyletic, and *Gerbekas*, *Heterocoelia*, *Parvoculus*, *Pycnomesitius*, *Sulcomesitius*, *Zimankos* were found to be polyphyletic. Two new genera are proposed and described: *Hadesmesitius* **gen. nov.** and *Brachymesitius* **gen. nov.**; *Botoryan* is considered as a junior synonym for *Zimankos*. Three species status are revalidated; and 11 species combinations were proposed, so that all genera are now monophyletic. The results indicate the thickness of integument in Mesitiinae could be related to their protection against their hosts.

Keywords

Biogeography, monophyletic, morphofunctional features, new genera, paraphyletic, polyphyletic, tribal classification

1. Introduction

The aculeate family Bethyridae includes nearly 3,000 species of parasitoid wasps, representing one of the most diverse lineages of Chrysoidea (Finnamore and Brothers 1993; Azevedo et al. 2018). Among bethyrids, the Mesitiinae have their diversity represented by 188 species distributed into 18 genera, recorded in tropical environments of the Afrotropical, Australian, Oriental, and Palearctic zoogeographical regions. Although many bethyrid fossils have been described in recent years (e.g., Azevedo and Azar 2012; Ramos et al. 2014; Colombo et al. 2021,

see also Azevedo et al. 2018 for a review), no fossil species of Mesitiinae were ever described. Known host records indicate that representatives of the subfamily are parasitoids of leaf-beetle larvae of the subfamilies Clytrinae and Cryptocephalinae (Coleoptera: Chrysomelidae), which reside in close-fitting cases built of fecal material (Argaman 2003). During oviposition, these wasps may exhibit predatory habits, since the female carries the paralyzed beetle immature into preexisting soil crevices with the mandibles (Nagy 1969; Argaman 2003).

Kieffer (1914) described Mesitiini as a tribe of Bethylinae, which was elevated to subfamily level by Berland (1928). The original description is very concise: “Of all the other different through the back corners of the metathorax, which protrude like teeth.” Only after five decades, Nagy (1969, 1972) proposed a redescription of the subfamily diagnosis based on several features, including body sculpture, eyes, dorsal pronotal area, mesonotum, metapetal-propodeal complex, forewings, and hypopygium. Móczár (1970a, 1971a) revised the two genera of Mesitiinae recognized at that time (*Heterocoelia* Dahlbom, 1854 and *Mesitius* Spinola, 1851) and redefined their diagnostic characteristics, describing seven new genera: *Anaylax* Móczár, 1970, *Incertosulcus* Móczár, 1970, *Metriorotus* Móczár, 1970, *Parvoculus* Móczár, 1970, *Pilomesitius* Móczár, 1970, *Pycnomesitius* Móczár, 1971 and *Sulcomesitius* Móczár, 1970. Nagy (1972) described the genera *Clytrovorus* Nagy, 1972, *Codorcas* Nagy, 1972 and *Topcobius* Nagy, 1972 based on features used by Móczár (1970, 1971) and added new ones from the hypopygium.

Argaman (2003) conducted a review of the Mesitiinae and proposed their division into four tribes: Domonkosini, Heterocoeliini, Mesitiini and Triglenusini. Additionally, he described seven new monotypic genera: *Botoryan* Argaman, 2003, *Domonkos* Argaman, 2003, *Gerbekas* Argaman, 2003, *Hamusmus* Argaman, 2003, *Itapayos* Argaman, 2003, *Ukayakos* Argaman, 2003 and *Zimankos* Argaman, 2003, for species previously included in other genera of the subfamily. He also revalidated *Topcobius*, previously considered a junior synonym of *Sulcomesitius* by Móczár (1984a), and transferred *Triglenus* Marshall, 1905 from Epyrinae to Mesitiinae. Argaman (2003) stated that his tribes were monophyletic but did not give a phylogenetic hypothesis.

The monophyly of the Mesitiinae was supported by the analyses in Sorg (1988), Carpenter (1999), Azevedo and Azar (2012) and Colombo et al. (2020); however, the internal phylogenetic relationships among included taxa have not been investigated so far. Moreover, we do not know how the diversification and phylogenetic relationships within Mesitiinae may have influenced their character transformations. Given this scenario, we investigated the character evolution of morphological features of Mesitiinae defined by former authors (i.e., Argaman 2003, Móczár 1970a, b, 1971a, b, 1984a, b, and Nagy 1969, 1972), aiming at providing a phylogenetic hypothesis about the relationship among the genera.

2. Material and methods

2.1. Collections

The specimens used in this study were borrowed from the following collections, with curators in parentheses:

NHM – The Natural History Museum, London, England (David Notton); **CASC** – California Academy of Sciences, San Francisco, U.S.A. (Robert Zuparko); **HNHM** –

Magyar Természettudományi Múzeum, Budapest, Hungary (Gellért Puskás); **MCSN** – Museo Civico di Storia Naturale “G. Doria”, Genova, Italy (Roberto Poggi); **MNHN** – Muséum National d’Histoire Naturelle, Paris, France (Claire Villemant); **MRAC** – Musée Royal de l’Afrique Centrale, Tervuren, Belgium (Eliane De Coninck); **QSBG** – Queen Sirikit Botanical Garden, Chiang Mai, Thailand (Wichai Srisuka); **UFES** – Universidade Federal do Espírito Santo, Vitória, Brazil (Celso Azevedo); **USNM** – National Museum of Natural History, Washington D.C., U.S.A. (David Furth); **ZMBH** – Museum für Naturkunde, Berlin, Germany (Frank Koch).

2.2. Illustrations

The images were obtained using a Leica MZ80 Stereomicroscope attached to a Leica DFC 495 video camera and captured with LEICA LAS (Leica Application Suite V3.6.0) by Leica Microsystems (Switzerland), using a dome illumination system described by Kawada and Buffington (2016), and combined using HELICON FOCUS (version 4.2.9). Illustrations and plates were edited for adjustments (e.g., levels, shadows/highlights).

2.3. Terminology

The terms applied to the structures follow Lanes et al. (2020) and Barbosa and Azevedo (2011), integument terminology follows Harris (1979). Abbreviation: VOL = vertex-ocular line in dorsal view.

2.4. Taxon sampling

The ingroup is composed by males of 61 species (Table 1). The species analyzed correspond to over a third of the 182 species in Mesitiinae. Species selection aimed to cover the maximum possible morphological diversity in each genus to facilitate possible taxonomic decisions. Character definition was based on males for three main reasons: (1) the current classification by Argaman (2003) was based on males; (2) the male hypopygium and genitalia offer a range of characters not available for females; and (3) lack of conspicuous sexual dimorphism between male and female.

Except for *Australomesitius* Barbosa & Azevedo, 2016, known only from the female, 17 out of the 18 genera currently included in the subfamily were sampled. The outgroup includes representatives of all extant subfamilies of Bethylinae (Table 1). The Bethylinae *Bethylus cephalotes* (Förster, 1860) was used for rooting the tree.

Table 1 should be included here associated with subchapter 2.4, landscape, and maximally page-filling.

2.5. Characters

A total of 112 characters (Appendix 1) were analyzed. Many of them were taken from descriptions in Móczár

Table 1. Specimens included in the phylogenetic analysis

Taxa	Specimen	Zoogeographic region	Repository
Ingroup (Mesitiinae)			
Domonkosini			
<i>Pilomesitius madagascarensis</i> Móczár, 1970	Allotype	Madagascar	MNHM
<i>Zimankos alluaudi</i> (Kieffer, 1913)	Allotype	Ethiopic	MRAC
<i>Zimankos makoa</i> Barbosa & Azevedo, 2012	Holotype	Madagascar	CASC
<i>Zimankos pondo</i> (Benoit, 1968)	Paratype	Ethiopic, Oriental	UFES
<i>Zimankos rieki</i> Móczár, 1976	Paratype	Oriental	HNHM
<i>Zimankos szentivanyi</i> Móczár, 1976	Paratype	Oriental	HNHM
<i>Zimankos vechti</i> Móczár, 1979	Paratype	Oriental	HNHM
Heterocoeliini			
<i>Botoryan discolor</i> (Nagy, 1968)	Holotype	Oriental	USNM
<i>Gerbekas carcelli</i> (Westwood, 1874)	Voucher	Palaeartic	MCSN
<i>Gerbekas laosensis</i> Móczár, 1975	Holotype	Oriental	HNHM
<i>Heterocoelia cursor</i> (Kieffer, 1906)	Allotype	Palaeartic	HNHM
<i>Heterocoelia fischeri</i> Móczár, 1971, jr. syn. of <i>Pycnomesitius peringueyi</i> (Kieffer, 1913)	Holotype	Ethiopic	MRAC
<i>Heterocoelia halidaiella</i> (Westwood, 1874)	Voucher	Palaeartic	HNHM
<i>Heterocoelia halidaii</i> (Westwood, 1874)	Voucher	Palaeartic	HNHM
<i>Heterocoelia hungarica</i> (Kieffer, 1906)	Voucher	Palaeartic	HNHM
<i>Heterocoelia nikolskajae</i> Móczár, 1984, jr. syn. of <i>H. obscura</i> (Kieffer, 1906)	Paratype	Palaeartic	UFES
<i>Heterocoelia obscurus</i> (Kieffer, 1906)	Neótipo	Palaeartic	HNHM
<i>Pycnomesitius benoitii</i> (Móczár, 1970)	Paratype	Ethiopic	UFES
<i>Pycnomesitius desenpunctatus</i> Móczár, 1971	Allotype	Ethiopic	BMNH
<i>Pycnomesitius peringueyi</i> (Kieffer, 1913)	Voucher	Ethiopic	HNHM
<i>Sulcomesitius kosztarabi</i> Móczár, 1984	Paratype	Oriental	HNHM
<i>Sulcomesitius nepalensis</i> Móczár, 1986	Paratype	Oriental	UFES
<i>Sulcomesitius punctaticollis</i> (Fouts, 1930)	Holotype	Oriental	USNM
<i>Sulcomesitius</i> sp.01	Voucher	Oriental	QSBG
<i>Sulcomesitius thailandensis</i> Móczár, 1977	Paratype	Oriental	HNHM
<i>Sulcomesitius wahisi</i> Móczár, 1984	Paratype	Oriental	HNHM
Mesitiini			
<i>Anaylax betsileo</i> Barbosa & Azevedo, 2012	Holotype	Madagascar	CASC
<i>Anaylax mahafaly</i> Barbosa & Azevedo, 2012	Holotype	Madagascar	CASC
<i>Anaylax simplicitus</i> Barbosa & Azevedo, 2011	Holotype	Ethiopic	UFES
<i>Astromesitius indistintus</i> Barbosa & Azevedo, 2011	Holotype	Ethiopic	UFES
<i>Astromesitius minutissimus</i> (Móczár, 1971)	Voucher	Ethiopic	UFES
<i>Astromesitius olavoii</i> Barbosa & Azevedo, 2019	Holotype	Oriental	QSBG
<i>Clytrovorus fuscicornis</i> (Kieffer, 1906)	Holotype	Palaeartic	HNHM
<i>Clytrovorus horvathi</i> (Kieffer, 1906)	Allotype	Palaeartic	HNHM
<i>Clytrovorus merina</i> (Barbosa & Azevedo, 2012)	Holotype	Madagascar	CASC
<i>Clytrovorus zafimaniry</i> Barbosa & Azevedo, 2012	Holotype	Madagascar	CASC
<i>Incertosulcus capensis</i> (Kieffer, 1911)	Allotype	Ethiopic	MRAC
<i>Incertosulcus consimilis</i> Móczár, 1970	Paratype	Ethiopic	UFES
<i>Incertosulcus krombeini</i> Móczár, 1970, jr. syn. of <i>Parvoculus indicus</i> Kieffer, 1913	Holotype	Palaeartic	BMNH
<i>Incertosulcus priesneri</i> Móczár, 1978	Holotype	Palaeartic	USNM
<i>Incertosulcus soikai</i> Móczár, 1970	Holotype	Palaeartic	HNHM
<i>Incertosulcus vanharteni</i> Barbosa & Azevedo, 2011	Holotype	Ethiopic	CNCI
<i>Incertosulcus vietnamensis</i> Móczár, 1977	Paratype	Oriental	HNHM
<i>Incertosulcus</i> sp.01	Voucher	Oriental	QSBG
<i>Itapayos antaimoro</i> Barbosa & Azevedo, 2012	Holotype	Madagascar	CASC
<i>Itapayos</i> sp.01	Voucher	Oriental	QSBG
<i>Mesitius granulata</i> Móczár, 1984	Holotype	Oriental	USNM
<i>Mesitius kiefferi</i> Nagy, 1970	Holotype	Palaeartic	ZMB
<i>Mesitius krombeini</i> (Nagy, 1968)	Holotype	Oriental	USNM
<i>Mesitius paenepunctata</i> (Benoit, 1968)	Holotype	Ethiopic	MCSN
<i>Metrionotus alutaceus</i> (Benoit, 1968)	Paratype	Ethiopic	UFES
<i>Metrionotus brevispinosus</i> (Benoit, 1968)	Paratype	Ethiopic	UFES

Taxa	Specimen	Zoogeographic region	Repository
<i>Metrionotus rufohumerus</i> Móczár, 1984	Paratype	Oriental	HNHM
<i>Metrionotus wolffi</i> Móczár, 1970	Paratype	Ethiopic	UFES
<i>Parvoculus indicus</i> (Kieffer, 1905)	Holotype	Oriental	HNHM
Triglenusini			
<i>Bradepyrus baleariensis</i> Barbosa & Azevedo, 2015	Voucher	Palaearctic	HNHM
<i>Bradepyrus dimorphus</i> (Kieffer, 1911)	Allotype	Palaearctic	BMNH
<i>Bradepyrus inermis</i> (Kieffer, 1906)	Allotype	Palaearctic	HNHM
<i>Bradepyrus jordanicus</i> Barbosa & Azevedo, 2015	Voucher	Palaearctic	HNHM
<i>Bradepyrus proximus</i> (Kieffer, 1906)	Holotype	Palaearctic	MNHN
<i>Moczariella centenaria</i> (Barbosa & Azevedo, 2014)	Holotype	Ethiopic	UFES
Outgroup			
<i>Bethylus cephalotes</i> Forster, 1860	Voucher	Palaearctic	UFES
<i>Goniozus legneri</i> Gordh, 1982	Voucher	Holarctic, Neotropical	UFES
<i>Chlorepyrus longifoveatus</i> (Azevedo, 1999)	Paratype	Neotropical	UFES
<i>Epyrus variatus</i> Córrea & Azevedo, 2002	Paratype	Neotropical	UFES
<i>Apenesia sahyadrica</i> Azevedo & Waichert, 2006	Paratype	Oriental	UFES
<i>Disssomphalus cervoides</i> Azevedo, 2003	Paratype	Neotropical	UFES
<i>Plastanoxus westwoodi</i> (Kieffer, 1914)	Voucher	Holarctic, Neotropical	UFES
<i>Sclerodermus irradiatus</i> (Lanes & Azevedo, 2004)	Paratype	Oriental	UFES

(1970, 1971), Nagy (1969, 1972), and Argaman (2003); additionally, new characters are proposed here for the first time.

2.6. Character matrix

The character matrix (Table S1) was produced using DELTA software (Dallwitz et al. 1993). All characters were treated as unordered. Inapplicable characters were coded as “?”.

2.7. Parsimony analyses

The searches for the most parsimonious trees were carried out in TNT version 1.5 (Goloboff et al. 2016, using the Ratchet, Sectorial Searches and Tree-Fusing searching strategies (Goloboff 1999, Nixon, 1999). Parameters were as follows: collapsing rules selected for TBR; random seed set to 0; Sectorial Search in default mode; 200 iterations of Ratchet; 20 cycles for Drift; 10 rounds for Tree Fusing.

It has been argued that results based on characters properly weighted are to be preferred over those with all characters equally weighted (Farris 1969, Goloboff 1993, Goloboff et al. 2008a). Implied weighting is the most widely used method for attributing different weights during tree search, as it is independent of previous analyses and weighting schemes unlike, for example, successive weighting (e.g., Farris 1969). The weighting against homoplasy under implied weighting is related to a constant k — the lower the value of k , the higher the strength against homoplasy Goloboff et al. (2008b). Here, we used the TNT script setk.run, written by Salvador Arias (Instituto Miguel Lillo, San Miguel de Tucuman, Argentina), to calculate the value of k . The script returned a value of $k = 11.674805$ for our data set.

2.8. Bayesian analyses

Bayesian analyses were conducted in MRBAYES 3.2.7 (Ronquist et al. 2012). We used the Mk model to morphological data, with correction for ascertainment bias (lset coding = variable), since autapomorphic characters were included. We first conducted an analysis without partitioning the original matrix, accounting for among-character rate heterogeneity using a discrete Gamma distribution with four rate categories (lset rates = gamma) and the prior on branch lengths described by an exponential distribution with scale parameter = 10 (prset brlenspr = Unconstrained:Exp(10)). We also conducted a similar analysis partitioning characters according to their degree of homoplasy. For this purpose, we retrieved homoplasy scores from implied-weighting analyses in TNT (see above). These values, derived from Goloboff’s measure of homoplasy, are normalized between 0 and 1, with the lowest value representing no homoplasy (Goloboff et al. 2008b). Branch lengths were maintained linked among partitions, and site-specific rates within partitions were not considered, as suggested by Rosa et al. (2019). MCMC analyses ran for 5,000,000 generations, sampling every 1,000, with four chains, and two independent runs. Convergence was assessed with Tracer 1.6 (Rambaut et al. 2018). Trees shown are majority-rule consensus trees (Contype = Allcompat).

3. Results

3.1. Cladistic analysis

The implied weighting analysis using $k = 11,674805$ resulted in one most parsimonious tree, with 675 steps, fit = 23,72727, consistency index (CI) = 0.19, and retention

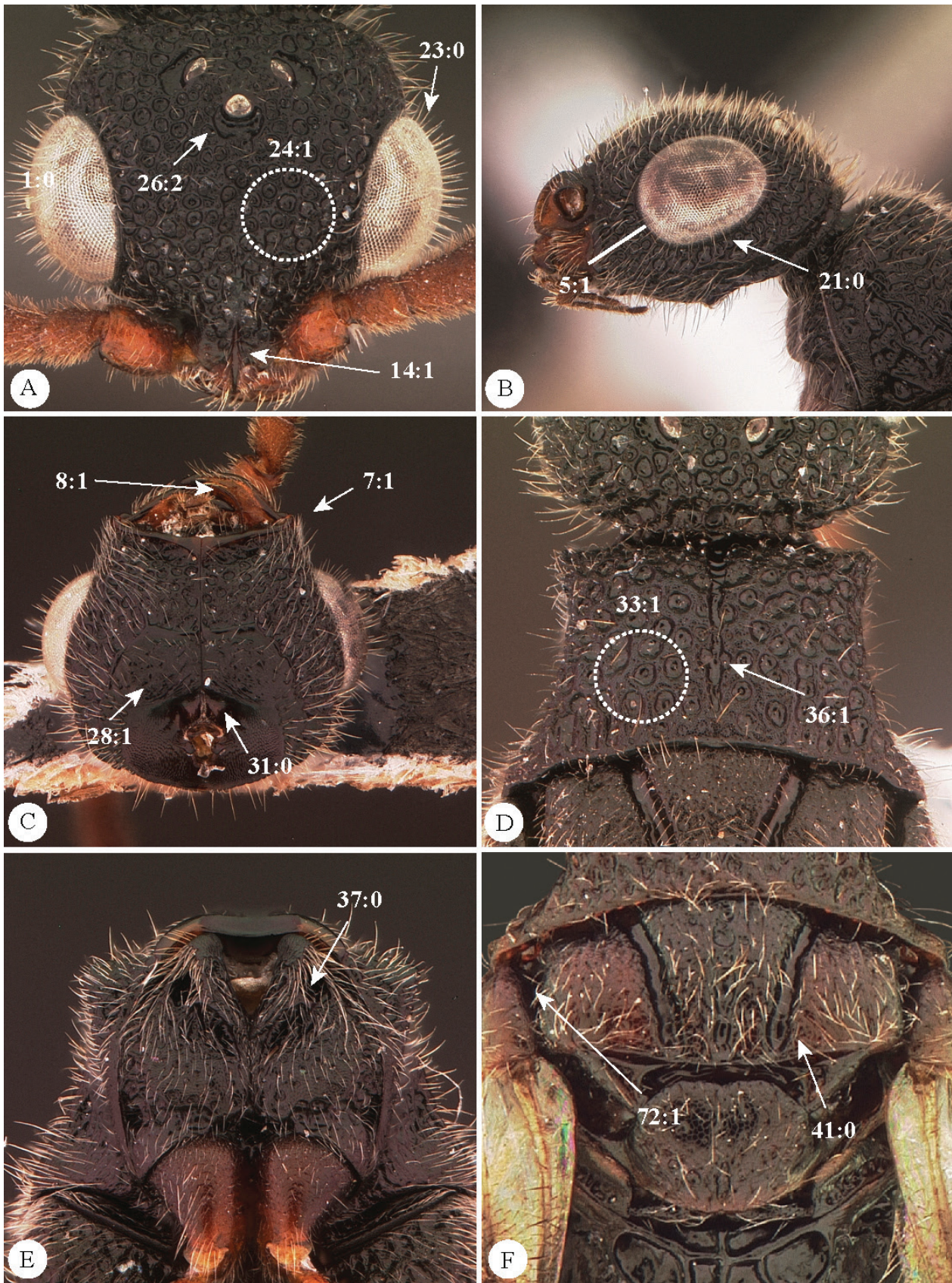


Figure 1. Characters and character states. **A** Head in dorsal view; **B** Head in lateral view; **C** Head in ventral view; **D** Pronotum in dorsal view; **E** Pronotum in ventral view; **F** Mesoscutum in dorsal view.

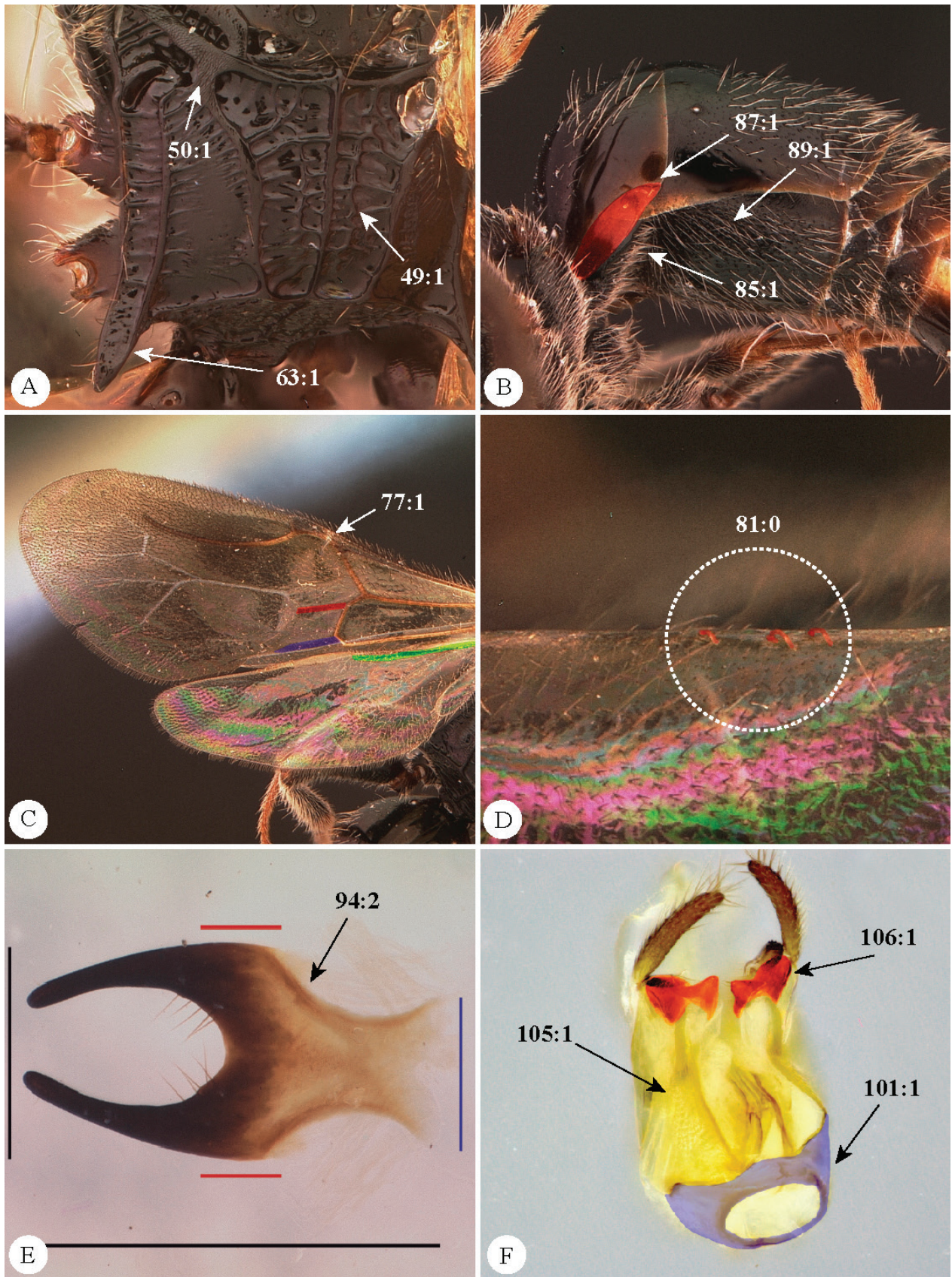


Figure 2. Characters and character states. **A** Metapectal-propodeal complex in dorsal view; **B** Metasoma lateral view; **C** Wings in dorsal view, red = nebulous cubital vein, blue = nebulous anal vein, green = subcostal vein; **D** Hind wing in dorsal view; **E** Hypopygium in ventral view; **F** Male genitalia in ventral view, red = cuspis, blue = genital ring.

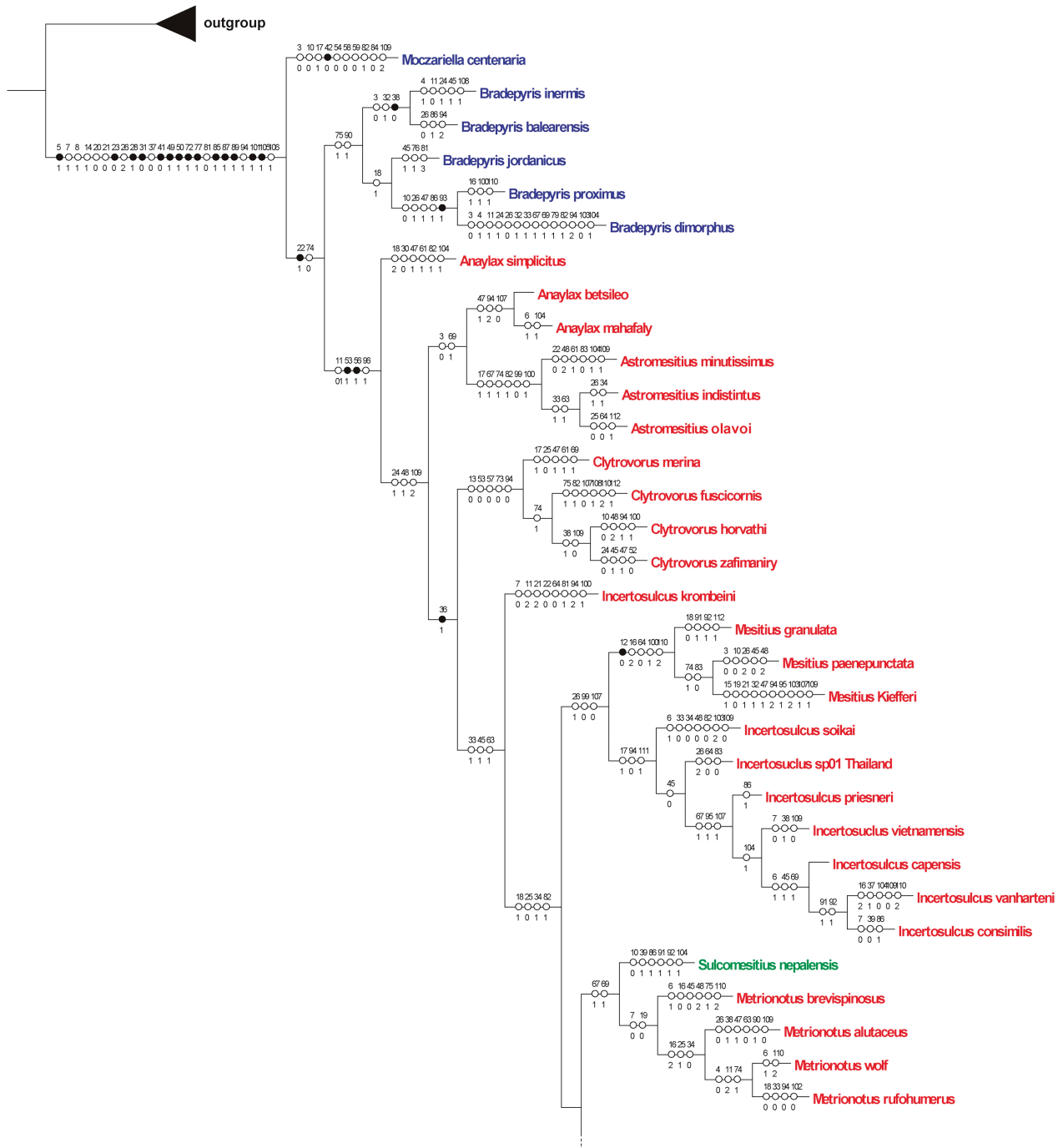


Figure 3. Part of the cladogram obtained with parsimony under implied weighting ($k = 11.674805$), showing characteristics and tribes sensu Argaman (2003). Blue = Trigenusini; red = Mesitiini; green = Heterocoeliini.

index (RI) = 0.61 (Figs 3–4; S1). The tribal classification proposed by Argaman (2003) was not supported, corroborating the classification taken by Azevedo et al. (2018).

Twenty-four characters were found as synapomorphies for the subfamily, 14 of them are exclusive transformations for Mesitiinae as listed below:

- Ch. 5:1 malar space projected (Fig. 1B);
- Ch. 23:0 contour of eye protruding (Fig. 1A);
- Ch. 28:1 anterior depression of occiput present (Fig. 1C);

- Ch. 31:0 ventral half of mesoccipital carina angled - (Fig. 1E);
- Ch. 41:0 notauli of mesoscutum convergent posteriorly (Fig. 1F);
- (Ch. 49:1 metapostnotal depression present (Fig. 2A);
- Ch. 50:1 connection between central depression and triangular lateral depression of metapectal-propodeal disc (Fig. 2A);
- Ch. 72:1 space between tegula and mesoscutum present (Fig. 1F);
- Ch. 77:1 prestigmal abscissa of radial 1 of forewing present (Fig. 2C);

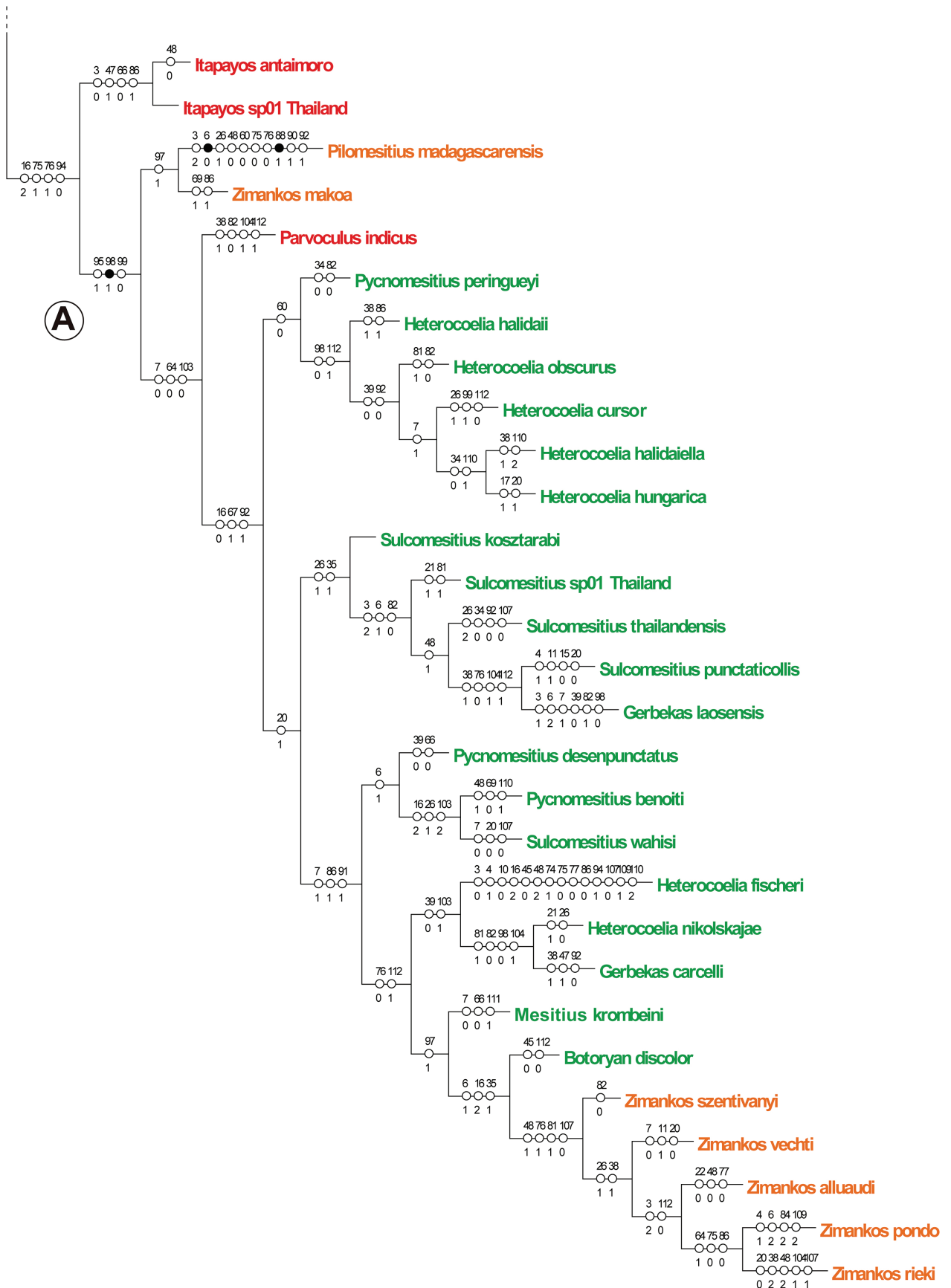


Figure 4. Part of the cladogram obtained with parsimony under implied weighting ($k = 11.674805$), showing characteristics and tribes sensu Argaman. Red = Mesitiini; orange = Domonkosini; green = Heterocoeliini.

Table 2. New nomina, nomenclatural acts and changes in combination in this study.

Original spelling/status	Current spelling/status	Spelling status
—	—	<i>Hadesmesitius</i> gen. nov.
—	—	<i>Brachymesitius</i> gen. nov.
<i>Anaylax simplicitus</i> Barbosa & Azevedo, 2011	<i>Anaylax simplicitus</i> Barbosa & Azevedo, 2011	<i>Hadesmesitius simplicitus</i> (Barbosa & Azevedo, 2011) comb. nov.
<i>Incertosulcus krombeini</i> Móczár, 1970	<i>Incertosulcus krombeini</i> Móczár, 1970	<i>Brachymesitius krombeini</i> (Móczár, 1970) comb. nov.
<i>Heterocoelia fischeri</i> Móczár, 1971	<i>Pycnomesitius fischeri</i> (Móczár, 1971) jun. syn. of <i>P. peringueyi</i> (Kieffer, 1913)	<i>Gerbekas fischeri</i> (Móczár, 1971) stat. rev. et comb. nov.
<i>Heterocoelia nikolskajae</i> Móczár, 1984	<i>Heterocoelia nikolskajae</i> Móczár, 1984 jun. syn. of <i>H. obscura</i> (Móczár, 1984)	<i>Gerbekas nikolskajae</i> (Móczár, 1984) stat. rev. et comb. nov.
<i>Sulcomesitius nepalensis</i> Móczár, 1986	<i>Sulcomesitius nepalensis</i> Móczár, 1986	<i>Metrionotus nepalensis</i> (Móczár, 1986) comb. nov.
<i>Sulcomesitius wahisi</i> Móczár, 1984	<i>Sulcomesitius wahisi</i> Móczár, 1984	<i>Pycnomesitius wahisi</i> Móczár, 1984 comb. nov.
<i>Heterocoelia laoensis</i> Móczár, 1975	<i>Gerbekas laoensis</i> (Móczár, 1975)	<i>Sulcomesitius laoensis</i> (Móczár, 1975) comb. nov.
<i>Botoryan</i> Argaman, 2003	<i>Botoryan</i> Argaman, 2003	<i>Botoryan</i> Argaman, 2003 syn. nov. of <i>Zimankos</i> Argaman, 2003
<i>Mesitius discolor</i> Nagy, 1968	<i>Botoryan discolor</i> (Nagy, 1968)	<i>Zimankos discolor</i> (Nagy, 1968) comb. nov.
<i>Zimankos makoa</i> Barbosa & Azevedo, 2012	<i>Zimankos makoa</i> Barbosa & Azevedo, 2012	<i>Pilomesitius makoa</i> (Barbosa & Azevedo, 2012) comb. nov.
<i>Mesitius krombeini</i> Nagy, 1968	<i>Mesitius krombeini</i> Nagy, 1968	<i>Zimankos krombeini</i> (Nagy, 1968) comb. nov.

- Ch. 85:1 constriction between metasomal sternite I and II present (Fig. 2B);
 Ch. 87:1 lateral ventral lap metasomal tergum I present (Fig. 2B);
 Ch. 89:1 metasomal segment II longer than others (Fig. 2B);
 Ch. 101:1 projection of genital ring present (Fig. 2F);
 Ch. 105:1 fusion between gonostipes and basivolsela present (Fig. 2F).

The other 10 characters states found as synapomorphies are not exclusive for Mesitiinae, but contributed to define the subfamily:

- Ch. 7:1 orientation of malar space parallel (Fig. 1C);
 Ch. 8:1 inner keel of mandible present (Fig. 1C);
 Ch. 14:1 torulus and median clypeal carina fused (Fig. 1A);
 Ch. 20:0 flagellomeres 1-11 slender (Fig. 1A);
 Ch. 21:0 eye small (Fig. 1B);
 Ch. 26:2 anterior ocellus crossing supra-ocular line (Fig. 1A);
 Ch. 37:0 anterior margin of propleuron angled (Fig. 1E);
 Ch. 81:0 hind wing with three distal hamuli (Fig. 2D);
 Ch. 94:1 hypopygium as long as wide (Fig. 2E);
 Ch. 106:1 cuspis with two arms (Fig. 2F).

3.2. Bayesian analyses

Bayesian analyses largely corroborated the backbone of the relationships retrieved in parsimony (Figs S2, S3). Results from unpartitioned and partitioned analyses dif-

ferred. In both analyses the genus *Anaylax* was not recovered as monophyletic, with *Anaylax simplicitus* being recovered as a distinct lineage relative to other species of the genus included in the present account. The unpartitioned analysis recovered *Incertosulcus krombeini* as sister group to *Metrionotus*, while in the analysis using partitioning by homoplasy score it was recovered nested within *Metrionotus*. However, the posterior probability of the clade *Metrionotus* + *I. krombeini* was very low in both cases (i.e., < 0.42). Both analyses also recovered different taxa as the sister group to all other mesitiine lineages: *Moczariella centenaria* in the unpartitioned analysis and the genus *Bradepyris* in the partitioned analysis.

3.3. Taxonomic Accounts

The interpretation of topologies obtained allowed us to propose 17 nomenclatural changes: two new genera, one genus synonymy, three revalidations in species status, and 11 new specific combinations (Figs 5–6; Table 2, S2). Because a recent review for diagnostic characteristics for Bethyridae genera was published by in Azevedo et al. (2018), we describe here only the diagnostic characteristics for the new genera proposed and the changes for the genera reinterpreted in this work.

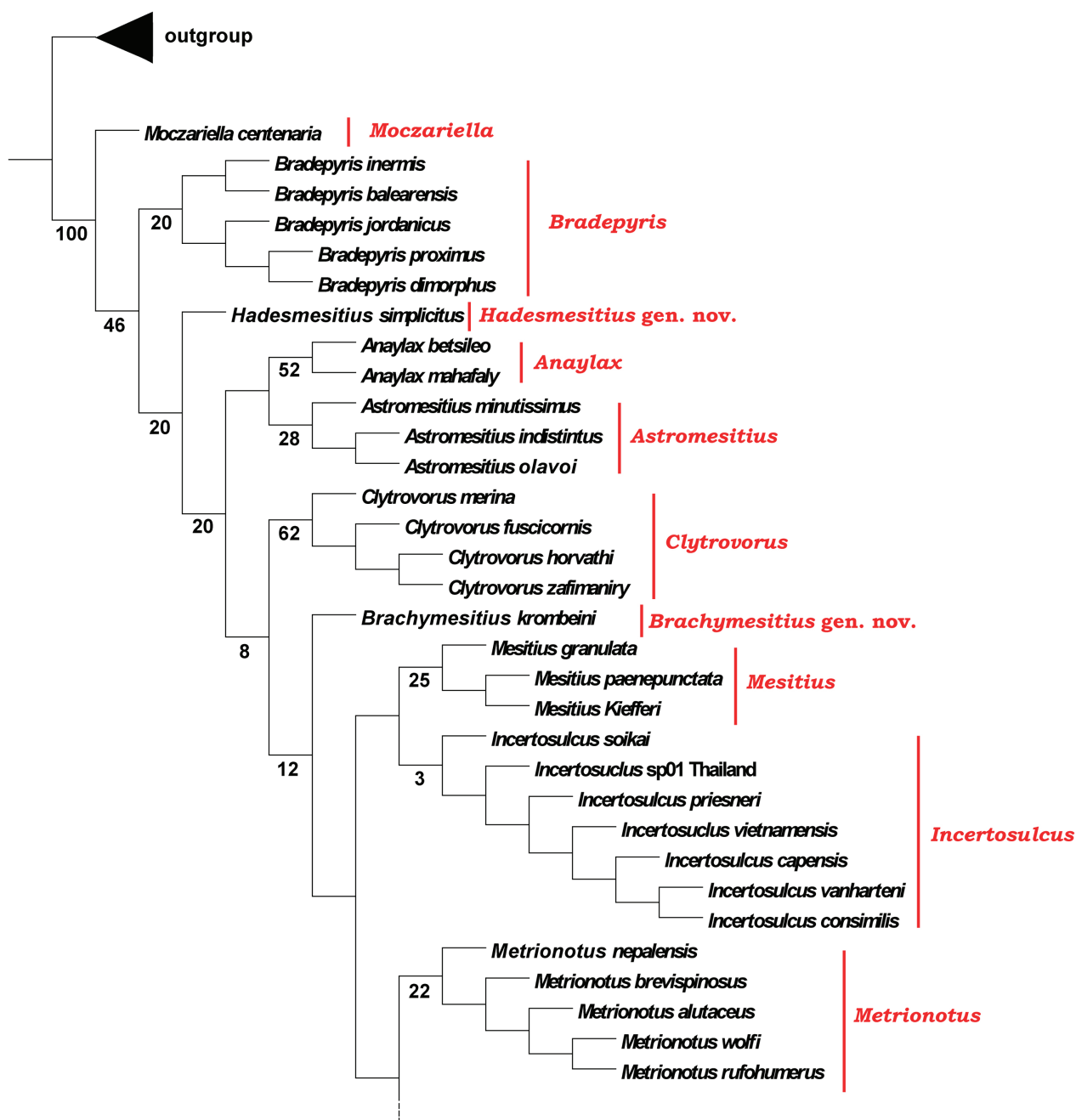


Figure 5. Part of the cladogram obtained with parsimony under implied weighting ($k = 11.674805$), showing newly proposed genera and symmetric resampling index.

3.3.1. New genera

***Hadesmesitius* Barbosa gen. nov.**

<http://zoobank.org/genus/E29C03A0-94C8-456D-B3B8-95487F4E3292>

Type species. *Anaylax simplicitus* Barbosa & Azevedo, 2011 by original designation.

Diagnosis. The length of first flagellomere shorter than pedicel (#18:2), ventral half of occipital carina absent (#30:0), mesoscutellum touching metapectal-propodeal disc (#47:1), propodeal spiracle circular (#61:1), distance

between distal hamuli and first hamuli more separated than others (#82:1), ventral arm of paramere of genitalia S-shaped (#104:1) are autapomorphies of *Hadesmesitius*. This genus has similarity with *Anaylax* and *Clytrovorus*, because they have the head, dorsal pronotal area and mesoscutum coriaceous, the median pronotal line and median mesonotal sulcus absent, and the posterior propodeal projection absent. Other characteristics also help to distinguish *Hadesmesitius* from *Anaylax* and *Clytrovorus*, as follows: hypopygium longer than wide and with filamentary branches, similar to *Pilomesitius*, *Pycnomesitius*, *Sulcomesitius*, and *Zimankos*; hind wing with distance between distal hamuli and first hamuli more separated than others, similar to *Zimankos*; and the ventral arm of paramere of genitalia S-shaped is shared with *Gerbekas*

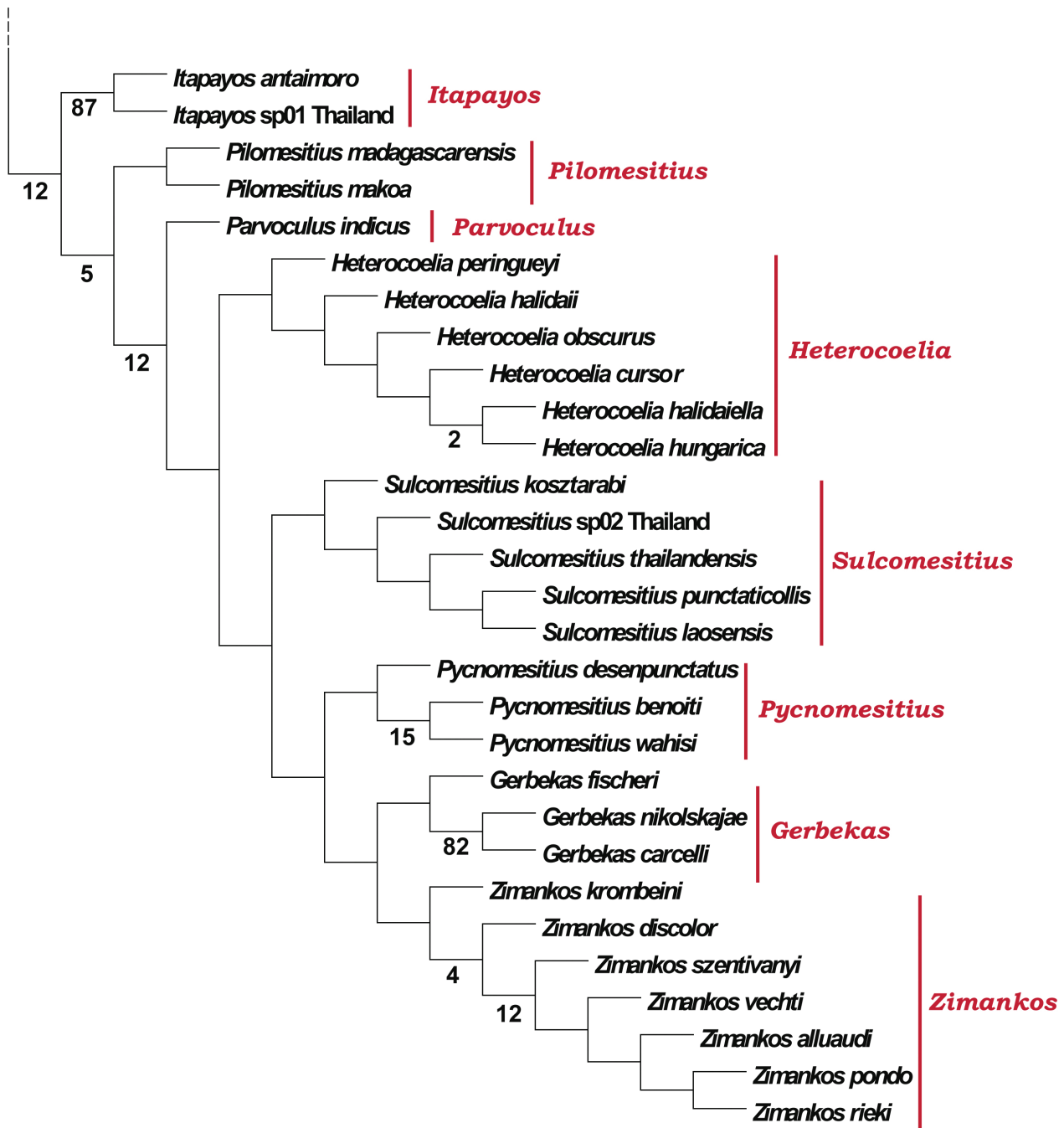


Figure 6. Part of the cladogram obtained with parsimony under implied weighting ($k = 11.674805$), showing newly proposed genera and symmetric resampling index.

and *Heterocoelia*. Based on comparisons with the other Mesitiinae genera and mainly on its monophyly, we introduce *Hadesmesitius* as a new genus for Mesitiinae.

Description. *Wings* subhyaline. *Head*: As long as wide; malar space shorter than VOL, parallel; clypeus with median lobe quadrate, median clypeal carina arched; antenna with pubescence sparse and short; pedicel fusiform, first flagellomere shorter than pedicel, flagellomeres long; eye small; frons not foveolate, with frontal carina; ocelli small; anterior ocellus posterior to supra-ocular line; dorsal half of occipital carina low, ventral half of occipital carina absent. *Pronotum*: Dorsal pronotal area shorter than wide, coriaceous, with humeral angle rounded, side

slightly incurved, anterior margin outcurved, posterior margin straight, median pronotal line absent; mesoscutum coriaceous, median mesonotal sulcus absent, notaulus narrow; mesoscutellum touching metapectal-propodeal disc; metapectal-propodeal disc as long as its half width, metapostnotal median carina incomplete, without longitudinal ridge between metapostnotal median carina and metapostnotal-propodeal carina, posterior propodeal projection absent; spiracle shape circular; propodeal declivity coriaceous and ecarinate; lateral surface of metapectal-propodeal complex coriaceous, without carinae. *Wings*: Hind wing with first hamuli more separated than others. *Metasoma*: Dorsal and ventral region of terga III–VI polished, with sparse setae at posterior

margin; hypopygium bilobate, spiculum as long as half of hypopygium, with filamentary and long branch, longer than wide, lateral margin parallel, corner angulate. **Genitalia:** With harpe dorsal arm shorter than ventral arm, 'S'-shaped, and with basal margin narrow, ventral arm of harpe wide apically; cuspis with distinct arms; aedeagus slender, with apex posterior to harpe apex, apical margin rounded, lateral of margin of basal portion slightly out-curved.

Etymology. The name *Hadesmesitius*, masculine, is a combination of the "Hades", the Greek mythology god that has a forked weapon with the same shape of the hypopygium in this genus, which is diagnostic for the group, and the name "*Mesitius*", the type genus of Mesitiinae.

Distribution. United Arab Emirates.

Species included. Only the type species *Anaylax simplicitus* Barbosa & Azevedo, 2011 in its current combination *Hadesmesitius simplicitus* (Barbosa & Azevedo, 2011) **comb. nov.**

***Brachymesitius* Barbosa gen. nov.**

<http://zoobank.org/genus/CBF4DC2A-6F41-4527-8168-8440C6044FA7>

Type species. *Incertosulcus krombeini* Móczár, 1970 by original designation.

Diagnosis. The malar space convergent (#7:0), apex of median clypeal carina [in profile] inclined (#11:2), eye very small (#21:2), pubescence of eye absent (#22:0), posterior propodeal projection wide (#64:0), number of distal hamuli of hind wing four (#81:1), hypopygium wider than long (#94:2), anterolateral hypopygial apodeme present (#100:1) were found to be autapomorphies for *Brachymesitius*. The type species was first described as a species of *Incertosulcus*. The genus was characterized by the presence or absence of a long posterior propodeal projection, making the identification dubious. Azevedo et al. (2018) proposed a new interpretation for the diagnostic characteristics for *Incertosulcus*, making *Incertosulcus krombeini*, as junior synonym of *Parvoculus indicus* Kieffer, 1905.

This genus shares similarities with *Anaylax*, *Clytrovorus*, and *Hadesmesitius* which have the head, dorsal pronotal area and mesoscutum coriaceous, and the median pronotal line and median mesonotal sulcus absent. Other characteristics distinguish *Brachymesitius* from *Anaylax*, *Clytrovorus*, and *Hadesmesitius*, including eyes very small, similar to *Bradepyrus* and *Moczariella*; the anterolateral hypopygial apodeme similar to *Mesitius*; and the hind wing with four distal hamuli is shared with *Zimankos*; the presence of frontal carina and the propodeal declivity and lateral surface of metapectal-propodeal complex areolate are exclusive for *Brachymesitius* as diagnostic characteristics.

Description. **Wings:** hyaline. **Head:** As long as wide; malar space as long as VOL, convergent; clypeus with median lobe rounded, median clypeal carina inclined; antenna with pubescence sparse and short; pedicel cylindrical, first flagellomere as long as pedicel, flagellomeres short; eye very small, without pubescence; frons foveolate, with frontal carina; ocelli very small; anterior ocellus crossing supra-ocular line; dorsal and ventral half of occipital carina low. **Pronotum:** Dorsal pronotal area shorter than wide, foveolate, with humeral angle rounded, side straight, anterior margin outcurved, posterior margin incurved, median pronotal line absent; mesoscutum coriaceous, median mesonotal sulcus absent, notaulus present and narrow; mesoscutellum not touching the metapectal-propodeal disc; metapectal-propodeal disc as long as its half width, metapostnotal median carina complete, with longitudinal ridge between metapostnotal median carina and metapostnotal-propodeal carina, posterior propodeal projection very short and thick; spiracle shape elliptical; propodeal declivity areolate, with median and lateral carinae; lateral surface of metapectal-propodeal complex areolate, without carinae. **Wings:** Hind wing with four distal hamuli. Metasoma dorsal and ventral region of terga III–VI polished; hypopygium bilobate, spiculum short, with lobate and short branch, wider than long, lateral margins convergent, with lateral anterior projection.

Etymology. The name *Brachymesitius*, masculine, is a combination of the names "brachy", from the Greek "short", and refers to the reduced size of structures, such as eye size, flagellomeres, ocelli, length of dorsal pronotal area, posterior propodeal projection, and hypopygium, which are diagnostic for the group, and the name "*Mesitius*", the type genus of Mesitiinae.

Distribution. Iraq.

Species included. *Incertosulcus krombeini* Móczár, 1970, now *Brachymesitius krombeini* (Móczár, 1970) **stat. rev. et comb. nov.**, removed from the synonymy of *Parvoculus indicus* Kieffer, 1905.

3.3.2. Notes on Mesitiinae genera

***Gerbekas* Argaman, 2003**

Remarks. This genus is characterized by the antenna with flagellomeres wide with pubescence dense and short, the forewing with nebulous Cu vein, the hypopygium with wide spiculum and branches lobate, and the male genitalia with parameres S-shaped (Azevedo et al. 2018). However, it was found to be polyphyletic (Figs 4–6). In order to solve this problem, *Heterocoelia fischeri* Móczár, 1971 is herein removed from the synonymy of *Pycnomesitius peringueyi* (Kieffer, 1913) and transferred to *Gerbekas*, *G. fischeri* (Móczár, 1971) **stat. rev. et comb. nov.**; and *Heterocoelia nikolskajae* Móczár, 1984 is herein removed from the synonymy of *Heterocoelia obscura* (Móczár,

1984) and also transferred to *Gerbekas*, *G. nikolskajae* (Móczár, 1984) **stat. rev. et comb. nov.**

Pycnomesitius Móczár, 1971

Remarks. This genus is characterized by the head as long as wide, the anteromesoscutum without median mesonotal line, the posterior propodeal projection short, and the metasomal tergum II densely punctured (Azevedo et al. 2018). However, it was found to be polyphyletic (Figs 4–6). In order to solve this problem, *Sulcomesitius wahisi* Móczár, 1984 is herein transferred from *Sulcomesitius* to *Pycnomesitius*, *P. wahisi* (Móczár, 1984) **comb. nov.**

Sulcomesitius Móczár, 1970

Remarks. This genus is characterized by the malar space as long as vertex-ocular line, convergent anteriorly, in front view, the anteromesoscutum with median mesonotal line well impressed, the forewing with nebulous Cu and A veins, the hypopygium with branches lobate and long, and the male genitalia with dorsal paramere S-shaped, ventral paramere narrower than dorsal (Azevedo et al. 2018). However, it was found to be polyphyletic (Figs 4–6). The same applies to *Sulcomesitius nepalensis*, which was recovered as sister group to a clade formed by four species of *Metrionotus* and *Brachymesitius krombeini* in the partitioned Bayesian analysis and recovered nested within species of *Metrionotus* in the unpartitioned analysis; and *Gerbekas laoensis*, which was recovered as sister group to a clade formed by four species of *Sulcomesitius* in the partitioned Bayesian analysis and as single clade in the unpartitioned analysis. In both cases, the support for such groupings is low, indicated by posterior probability values below 0.4. To solve this problem, *Sulcomesitius nepalensis* Móczár, 1986 is herein transferred to *Metrionotus*, *M. nepalensis* (Móczár, 1986) **comb. nov.** and *Gerbekas laoensis* Móczár, 1975 is herein transferred from *Gerbekas* to *Sulcomesitius*, *S. laoensis* (Móczár, 1975) **comb. nov.**

Zimankos Argaman, 2003

Remarks. This genus is characterized by the malar space with sides parallel and as long as vertex-ocular line, the antennal pubescence dense and mid-sized (about 0.5 × flagellomeral width), the dorsal pronotal area with humeral angle projected, the hind wing with four hamuli, and the hypopygium with wide spiculum and long branches (Azevedo et al. 2018). However, it was found to be polyphyletic (Figs 4–6). In order to solve this problem, several nomenclatural changes were needed, including: *Botoryan* **syn. nov.** is synonymized with *Zimankos* and its single species *B. discolor* (Nagy, 1968) is transferred to *Zimankos*, as *Zimankos discolor* (Nagy, 1968) **comb. nov.** *Zimankos makoa* Barbosa & Azevedo, 2012 is herein transferred to *Pilomesitius*, *P. makoa* (Barbosa & Aze-

vedo, 2012) **comb. nov.**; the same for *Mesitius krombeini*, which was recovered as sister group to a clade formed by four species of *Gerbekas* and *Heterocoelia* in the unpartitioned and partitioned Bayesian analysis. In both cases, the support for such groupings is low, indicated by posterior probability values below 0.4; thus, *Mesitius krombeini* Nagy, 1968 is herein transferred to *Zimankos*, *Zimankos krombeini* (Nagy, 1968) **comb. nov.**

4. Discussion

4.1. Phylogenetic inference

Argaman (2003) mentions that the posterior oblique sulcus of mesopleuron was an autapomorphy for Mesitiinae, but this was not found as a subfamily synapomorphy. From twenty-five subfamily diagnostic features defined by Azevedo et al. (2018), eight were found as synapomorphies: malar space projected (#5:1); inner keel of mandible present (#8:1); torulus and median clypeal carina fused (#14:1); eye small (#21:0); contour of eye protruding (#23:0); anterior depression of occiput present (#28:1); anterior margin of propleuron angled (#37:0); notauli convergent posteriorly (#41:0). The metapostnotal depression present (#49:1), metapostnotal depression and paraspiracular sulcus metapectal-propodeal disc present (#50:1), space between tegula and mesoscutum present (#72:1), and anterior margin of propleuron angled (#37:0) were found as synapomorphies for the first time. The metasomal segment II longer than others the only feature previously found as a Mesitiinae synapomorphy, by Sorg (1988).

Although Argaman (2003) stated that his tribal classification was based on monophyletic grouping, he did not publish this phylogenetic analysis, and analyses by Azevedo et al. (2018) did not support his results. Argaman (2003) described Triglenusini based on the characters shared by *Bradepyris* Kieffer, 1905, *Pseudomesitius* (Duchaussoy, 1916 [1914], and *Triglenus* Marshall, 1905. The two latter genera were treated as junior synonyms of *Bradepyris* by Barbosa & Azevedo (2015), and our analysis showed that Triglenusini is a paraphyletic grouping. The Mesitiini were described based on the characters shared by *Anaylax* Móczár, 1970a, *Clytrovorus* Nagy, 1972, *Incertosulcus* Móczár, 1970aa, *Itapayos*, *Mesitius* Spinola, 1853, *Metrionotus* Móczár, 1970a and *Parvoculus* Móczár, 1970d, and were recovered as polyphyletic in our analysis. The Heterocoeliini were described based on characters shared by *Botoryan*, *Codorcas* Nagy, 1972 (junior synonym of *Heterocoelia*), *Gerbekas*, *Hamasmus* (junior synonyms of *Heterocoelia*), *Heterocoelia* Dahlbom, 1854, *Pycnomesitius* Móczár, 1971b, *Sulcomesitius* Móczár, 1970c and *Ukayakos* (junior synonyms of *Heterocoelia*); however, Heterocoeliini were not supported as a monophyletic group, being recovered as polyphyletic instead. The tribe Domonkosini was based on characters shared by *Domonkos* (junior synonym of *Incertosulcus*),

Pilomesitius Móczár, 1970b, *Topcobius* Nagy, 1972 (junior synonym of *Sulcomesitius*) and *Zimankos*, and was not supported as a monophyletic group, the evidence indicating that *Domonkosini* are a polyphyletic grouping. The same relationships were also observed in the Bayesian analysis. Therefore, we corroborate the decision of Azevedo et al. (2018) and maintain Mesitiinae without tribal classification.

Among genera represented by more than one terminal in parsimony analyses, five were found to be monophyletic: *Astromesitius* Barbosa & Azevedo, 2019, *Bradepyris*, *Clytrovorus*, *Itapayos*, and *Mesitius*; three were found to be paraphyletic: *Botoryan*, *Metriorotus*, and *Pilomesitius*; and eight were found to be polyphyletic: *Anaylax*, *Gerbekas*, *Heterocoelia*, *Incertosulcus*, *Parvovulus*, *Pycnomesitius*, *Sulcomesitius*, and *Zimankos*. Additionally, the paraphyly of *Metriorotus* and *Pilomesitius* and the polyphyly of *Gerbekas*, *Heterocoelia*, *Pycnomesitius*, *Sulcomesitius*, and *Zimankos* required new combinations (see below). *Botoryan* was found forming a clade nested within *Zimankos* and therefore we treat it as junior synonym of the latter. *Anaylax simplicitus* Barbosa & Azevedo, 2011 and *Incertosulcus krombeini* Móczár, 1970 were both recovered as distinct lineages, not clustering with other species of their respective genera. *Mesitius krombeini* was retrieved as closely related to the clade formed by *Zimankos* + *Botoryan*. *Sulcomesitius nepalensis* Móczár, 1986 clustered with species of *Metriorotus*. *Gerbekas laosensis* Móczár, 1975 was recovered as related to four species of *Sulcomesitius*.

The topologies obtained allowed the identification of morphological characters which potentially played important roles during the diversification of Mesitiinae, including sculpture of frons (#24); sculpture of dorsal pronotal area (#33); presence of median pronotal line (#36); presence of posterior propodeal projection (#63); length of hypopygium (#94); shape of posterior hypopygeal margin (#96); and length of hypopygium branches (#98). These characters are unique to the subfamily and allow us to hypothesize about their evolution. These hypotheses are largely based on convergent characteristics shared between Mesitiinae and Chrysidinae (Chrysididae) (Argaman, 2003).

4.2. Integumental adaptations

From the 19 genera proposed for Mesitiinae, 15 exhibit roughly sculptured frons (character #24, state 1) and pronotal area (character #33, state 1), with foveolate patterns (Figs 1A, D), while only two genera completely lack these features. Mesitiinae attack beetle larvae of Chrysomelidae (Coleoptera) (Argaman 2003), the author found them living into ant nets, hence the thick and robust integument of Mesitiinae is presumably associated with the lifestyle of hosts. Michener (2000) postulated that the rough sculpturation (lamellae, carinae and foveolation) and projections could be related to the strengthening of the integument, providing defensive mechanisms for vulnerable areas such as the neck, base of metasoma, and

other membranous regions in kleptoparasitic bees. Similar integumental sculpturation is observed in Nyssonini (Crabronidae), a group of apoid wasps that also exhibit kleptoparasitic behavior (Bohart and Menke 1976) and Chrysidinae (Chrysididae), which attack bees and aculeate wasps (Kimsey 1992). The same and convergent features can be observed in Mutillidae (Ronchetti and Polidori 2020). Thus, the integumental thickening in Mesitiinae seems to be associated with defense against their aculeate hosts, as mentioned by Lucena and Almeida (2022?) for Chrysidinae.

Cryptocephalini and Clytrini (Cryptocephalinae) leaf beetles have close association with ant nests. The larval stages remain in the ant nest in a positive interaction. The cocoon brought by the beetle mother is carried by the ants into the nest to complete its development (Agrain et al. 2015). Thus, to reach their beetle hosts, the Mesitiinae need to enter the ant nests. The convergent behavior among all taxa above is that all of them have dangerous hosts (bees and ants), as cited Thus, dense foveolation and thick integument could be associated with defenses.

4.3. Relation between pronotal structure and head movements

The median pronotal line (Character #36, state 1) characteristic of many mesitiine lineages (Fig. 1D) is associated with the pronotum-postoccipital muscle (Vilhelmsen et al. 2010), which has its origin at the internal ridge associated with this impression. This ridge could increase the anchorage insertion point allowing stronger contractions. The muscle is the pronotal elevator of the head, so the increase of power for this muscle allows more possibilities for head movements. Nagy (1968) described the parasitoid behavior of females of Mesitiinae and recorded that they steal pre-pupal beetles from the ant nests using their mandibles. Therefore, the increased range of head movements could be adaptive in the context of the female parasitoid behavior.

4.4. Propodeal adaptations

Among bethylids, the posterior projections on the propodeum (Fig. 2A) are exclusive for Mesitiinae (Character #63, state 1). However, it is absent in *Anaylax*, *Astromesitius*, *Bradepyris*, *Clytrovorus*, *Hadesmesitius* **gen. nov.**, and *Moczariella*. Argaman (2003) argued that this posterior projection could facilitate the opening of the cocoon wall during adult emergence, but this was never confirmed for Mesitiinae species. Perhaps a more plausible hypothesis is that the posterior propodeal projection is associated with defense against ants, with the projection protecting the base of metasoma, preventing damage to the petiole.

On the other hand, the musculature could indicate another adaptation associated with this structure. The muscle T1-S/T2 has its origin at the posterior corner of the metapectal-propodeal complex and inserts at anterior

margin of second metasomal segment. We dissected some Mesitiinae specimens with this projection and observed that the T1-S/T2 muscle has its origin inside the projection, thus increasing the anchorage insertion point of this muscle and giving it more strength. Additionally, this muscle is related to the sternal torsion of the metasoma (Mikó et al. 2007).

All mesitiine wasps have the second metasomal segment longer than the others, an exclusive feature for the subfamily (Barbosa and Azevedo 2011), which was also recovered herein as a synapomorphy for Mesitiinae. The great degree of metasomal segment modification, mainly the length of the third segment longer than others, is associated with oviposition, copulation and defense. Moreover, an additional muscle row was recorded in association with this segment expansion (Kimsey 1992), which is an additional anchorage point for the T1-S/T2 muscle into the posterior propodeal projection.

4.5. Hypopygium modifications

There are several shapes of hypopygium exclusive to Mesitiinae, which are described by seven characters in the present analyses (Characters #94 to #100).

Clade A (Fig. 4 and 6) includes seven genera, comprising 113 described species, which represent 63.8% of the total diversity of the subfamily. In this clade are also included the largest species of Mesitiinae.

Muscles located at the base of male genitalia are responsible for movements such as protraction as well as copulation, being inserted at the anterior region of the hypopygium, including the spiculum and anterolateral apodeme. Therefore, the contraction and relaxation between the genitalia base and the spiculum provides the movement of genitalia structures. Thus, the shape and size of the spiculum have direct association with insertion of muscles in the genitalia, affecting the kind and potential of its movements that is, with more and diversified muscle insertions, structures will be capable of performing more complex movements.

The modification of the length of the hypopygial branches is associated with the deformation of the hypopygium, which results from the contraction of the muscles. More muscles inserted at a longer spiculum promote a higher degree of hypopygium deformation, hence the long branches are associated with long median indentation, providing the hypopygium with an area of deformation, giving the structure more flexibility. This is also associated with a wide spiculum. On the other hand, short branches are associated with a simple acute spiculum, since the muscle contraction provides less deformation to the hypopygium, without the need of a deformation area.

The hypopygium shape is associated with muscle insertion and hence it could provide specific functions and adaptations for each genus. Schulmeister (2003) recognized these muscles and named them as “a”, “b” and “c”. These muscles originate in the gonocondyle in the cupula and inserts at the spiculum and laterally at the ninth sternite (= hypopygium). The cupula is attached to the

male genitalia base, and the muscles among these sclerites promote some movement of the genitalia, thus the muscles gonocondyle-spiculum (a), laterally of gonocondyle-spiculum (b), and gonocondyle-laterally ninth sternite (c), have indirect action in male genitalia action (Schulmeister 2003). These muscles expose the male genitalia by the elevation of the basal margin of the cupula (Boudinot 2013), thus probably a larger insertion point could increase the torque movement.

4.6. Distribution and biogeography

Presently, Mesitiinae are known from warm regions of the Old World, encompassing all of its four zoogeographical regions: Afrotropical (including Madagascar), Australian, Oriental, and Palearctic (Fig. 7). Unfortunately, *Australomesitius mirus* Barbosa & Azevedo, 2006, the single species of the family ever recorded in Australia, could not be included in this analysis. However, its position can be inferred based on the shape of the apex of median clypeal carina, arched [in profile], the presence of fusion between sublateral and inner discal carina of propodeal disc, and the orientation of inner discal carina of propodeal disc not parallel with median carina. Observing the distribution patterns among Mesitiinae lineages, there is an apparent association of the early-diverging lineages (e.g., the genera *Bradepyris* and *Moczariella*) with the Palearctic region. Additionally, thirteen of nineteen Mesitiinae genera have species recorded from the Palearctic region. From the remaining six genera, *Australomesitius* is endemic of Australia and *Pilomesitius* is endemic of Madagascar, while the other four are recorded in the Oriental and Afrotropical regions.

Based on this pattern, it may be that the early diversification of Mesitiinae occurred in the Palearctic region, with lineages progressively occupying the adjacent Oriental and Afrotropical regions and, later, Australia and Madagascar. Occupation of Madagascar likely occurred several times independently within the subfamily, while only a single lineage was able to reach Australia. In the future, a dated phylogeny of the family allied to the exploration of its relationships among other bethylid lineages and discoveries regarding fossil history may provide valuable evidence for a detailed approach on biogeography and diversification of Mesitiinae.

5. Conclusions

The present study is the most comprehensive cladistic treatment focusing on Mesitiinae tribal classification and character evolution, and the first to treat a large representative group and more accurate classification for each tribe.

Triglenusini were recovered as paraphyletic, and Domonkosini, Heterocoeliini and Mesitiini as polyphyletic, showing the classification in Argaman (2003) as un-

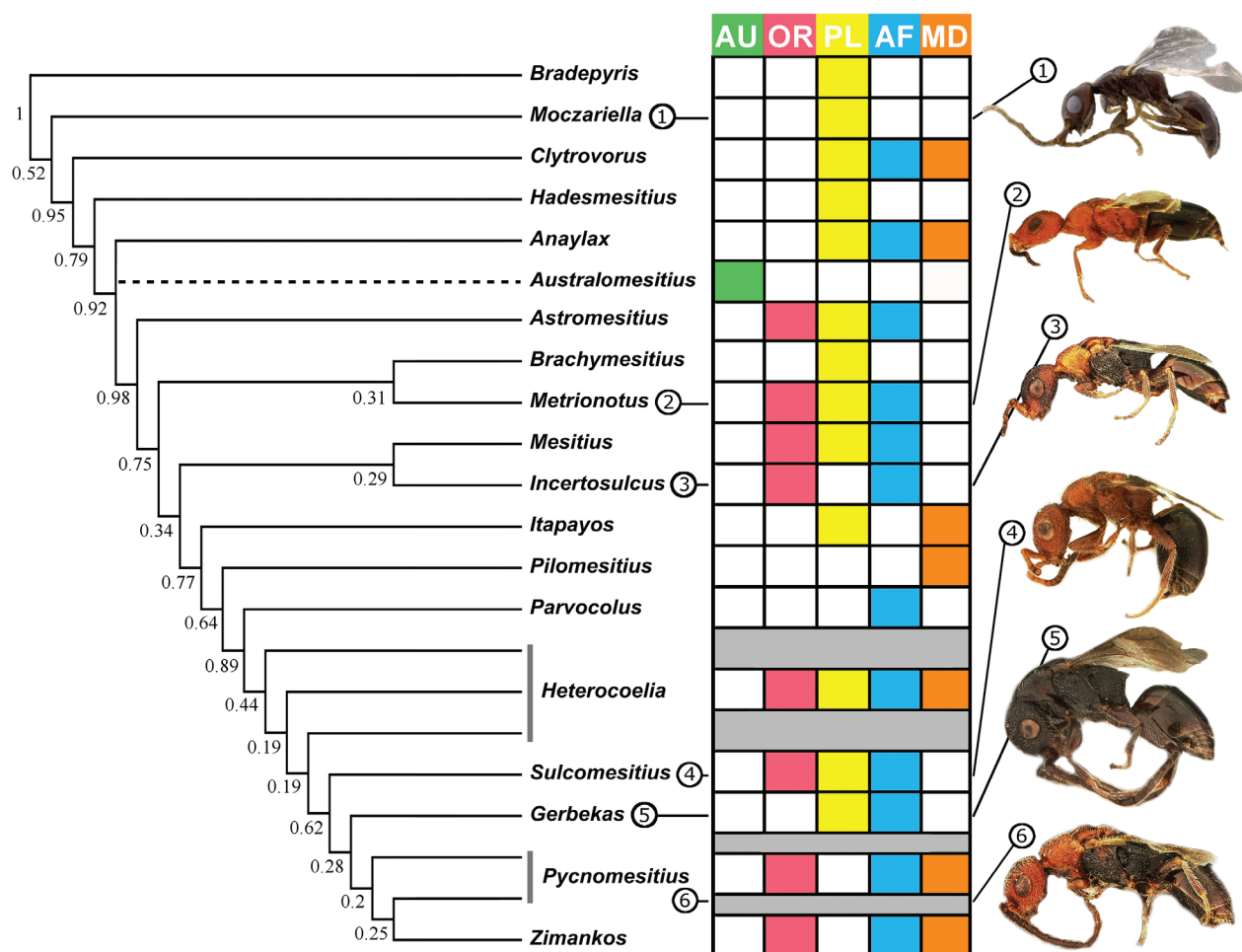


Figure 7. Cladogram showing the relationships among genera of Mesitiinae (according to the taxonomic treatment adopted herein), branching support, and their geographic distributions. Colored squares indicate presence on the respective regions: AU – Australia; OR – Oriental; PL – Palearctic; AF – Aftropical; MD – Madagascar. Position of *Australomesitius* is inferred based on characters mentioned in the main text. **1** *Moczariella centenaria*; **2** *Metrionotus yarrowi*; **3** *Incertosulcus priesneri*; **4** *Sulcomesitius bicolor*; **5** *Gerbekas fischeri*; **6** *Zimankos krombeini*.

ported. Morphological characters previously used in the former studies (Nagy 1969, 1972; Móczár 1970, 1971) were shown to be inconsistent regarding the monophyly of tribes. Thus, we corroborate the elimination of tribal treatment, following Azevedo et al. (2018).

6. Authors' contributions

DNB. planned, prepared, and designed the study. MH. and AL. supervised the study. DNB. performed the photography. DNB and MH. Performed the cladistic analyzes, AL. performed the Bayesian analyzes. DNB. described and recognized the new taxa. DNB. wrote the first draft of the manuscript. DNB., MH. and AL. discussed the results and revised the manuscript. All authors have read and approved the final version of the manuscript.

7. Competing interests

The authors have declared that no competing interests exist.

8. Acknowledgments

We thank the curators of the museums listed for providing the material required for this study, Géllert Puskás and Sándor Csósz for hosting DNB at HNHM, Celso O. Azevedo for being the main advisor to DNB during this study and facilitating access to the laboratory structure; thanks also to Geane Lanes, Ricardo Kawada, Fernando Noll, and Yuri Leite for careful revisions of the manuscript; to the Ernest Mayr Grant (Harvard Extension School) for funding the trip to HNHM in Budapest. This work was supported by CNPq #473386/2008-9, #620064/2006-4, Programa de Capacitação em Taxonomia #563953/05-5, FAPES #3935842/2007, #41106407/2008, and The Ernst Mayr Travel Grants in Animal Systematics, The Museum of Comparative Zoology (MCZ), Harvard University (2001). DNB received a scholarship from Programa de Capacitação em Taxonomia #562224/2010-6.

9. References

Agrain FA, Buffington ML, Chaboo CS, Chamorro ML, Schöller M (2015) Leaf beetles are ant-nest beetles: the curious life of the ju-

- venile stages of case-bearers (Coleoptera, Chrysomelidae, Cryptoccephalinae). In 'Research on Chrysomelidae 5'. (Eds P. Jolivet, J. Santiago-Blay and M. Schmitt.). ZooKeys 547: 133–164. <https://doi.org/10.3897/zookeys.547.6098>
- Argaman Q (2003) Generic synopsis of Mesitinae Kieffer, 1914 (Hymenoptera: Bethylinidae). Entomofauna 24: 61–96.
- Azevedo CO, Alencar IDCCA, Ramos MS, Barbosa DN, Colombo WD, Vargas JM, Lim J (2018) Global guide of the flat wasps (Hymenoptera, Bethylinidae). Zootaxa 4489: 1–294. <https://doi.org/10.11646/zootaxa.4489.1.1>
- Azevedo CO, Azar D (2012) A new fossil subfamily of Bethylinidae (Hymenoptera) from the Early Cretaceous Lebanese amber and its phylogenetic position. Zoologia 29: 210–218. <https://doi.org/10.1590/S1984-46702012000300004>
- Barbosa DN, Azevedo CO (2011) Order Hymenoptera, family Bethylinidae, subfamily Mesitiinae. In: Van Harten A (Ed) Arthropod Fauna of UAE Vol 4. Dar Al Ummah Printing, Publishing, Distribution & Advertising, Abu Dhabi, 375–404.
- Barbosa DN, Azevedo CO (2015) Synopsis of *Bradepyrus* Kieffer, 1905 (Hymenoptera, Bethylinidae, Mesitiinae). European Journal of Taxonomy 151: 1–16. <http://dx.doi.org/10.5852/ejt.2015.151>
- Berland L (1928) Hyménoptères Vespiformes II. In: Faune de France 19. Central de Faunistique, Paris, 1–215.
- Bohart RM, Menke AS (1976) Sphecid wasps of the world. A generic revision. University of California Press, Berkeley, Los Angeles, 695 pp.
- Boudinot BE (2013) The male genitalia of ants: musculature, homology, and functional morphology (Hymenoptera, Aculeata, Formicidae). Journal of Hymenoptera Research 30: 29–49. <https://doi.org/10.3897/JHR.30.3535>
- Carpenter JM (1999) What do we know about Chrysidoid (Hymenoptera) relationship? Zoologica Scripta 28: 215–231. <https://doi.org/10.1046/j.1463-6409.1999.00011.x>
- Colombo WD, Perkovsky EE, Azevedo CO (2020) Phylogenetic overview of flat wasps (Hymenoptera, Bethylinidae) reveals Elektroepyrinae, a new fossil subfamily. Palaeoentomology 3(3): 269–283. <https://doi.org/10.11646/palaeoentomology.3.3.8>
- Colombo WD, Perkovsky EE, Waichert C, Azevedo CO (2021) Synopsis of the fossil flat wasps Epyrinae (Hymenoptera, Bethylinidae), with description of three new genera and 10 new species. Journal of Systematic Palaeontology, 19(1), 39–89. <https://doi.org/10.1080/14772019.2021.1882593>
- Dahlbom AG (1854) Hymenoptera Europaea Praecipue Borealia. Berlin.
- Dallwitz MJ, Paine TA, Zurcher EJ (1993) User's Guide to the DELTA System: a General System for Processing Taxonomic Descriptions. Version 1.0.2 available online at <https://github.com/AtlasOfLiving-Australia/open-delta> (accessed in 6 march 2022).
- Duchaussoy A (1916) Nouveaux Bethylinides de l'Afrique du Nord et de l'Europe orientale (Hyménoptères). Societe d'Histoire Naturelle de Afrique du Nord. Bulletin 7: 109–126.
- Finnamore AT, Brothers DJ (1993) Superfamily Chrysidioidea. In: Goulet H, Huber JT (Eds) Hymenoptera of the world: an identification guide to families. Agriculture Canada Publications, Ottawa, 130–160.
- Goloboff PA (1993) Estimating character weights during tree search. Cladistics 9: 83–91. <https://doi.org/10.1111/j.1096-0031.1993.tb00209.x>
- Goloboff PA (1999) Analyzing large data sets in reasonable times: solutions for composite optima. Cladistics 15: 415–428. <https://doi.org/10.1111/j.1096-0031.1999.tb00278.x>
- Goloboff PA, Carpenter JM, Arias JS, Esquivel DRM (2008a) Weighting against homoplasy improves phylogenetic analysis of morphological data sets. Cladistics 24: 758–773. <https://doi.org/10.1111/j.1096-0031.2008.00209.x>
- Goloboff PA, Farris JS, Nixon KC (2008b) TNT, a free program for phylogenetic analysis. Cladistics 24: 774–786. <https://doi.org/10.1111/j.1096-0031.2008.00217.x>
- Goloboff, PA, Santiago CA (2016) TNT version 1.5, including a full implementation of phylogenetic morphometrics. Cladistics 32: 221–238. <https://doi.org/10.1111/cla.12160>
- Harris RA (1979) A glossary of surface sculpturing. Occasional Papers in Entomology 28: 1–31.
- Kawada R, Buffington ML (2016) A scalable and modular dome illumination system for scientific microphotography on a budget. PLoS One 11(5): e0153426. <https://doi.org/10.1371/journal.pone.0153426>
- Kieffer JJ (1905) Description de nouveaux Proctotrypi des exotiques avec une planche et une figure dans le texte. Annales Societe scientifique de Bruxelles 29: 95–142.
- Kieffer JJ, Marshall AK (1905) Proctotrypides. In: André E (Ed) Species des Hyménoptères d'Europe & d'Algerie Tome IX. Librairie Scientifique A. Hermann, Paris, 1–55.
- Kieffer JJ (1914) Bethylinae. Das Tierreich 41: 228–595.
- Kimsey LS (1992) Functional Morphology of Abdomen and Phylogeny of Chrysidid Wasps (Hymenoptera: Chrysididae). Journal of Hymenoptera Research 1(1): 165174.
- Lanes GO, Kawada R, Azevedo CO, Brothers D (2020) Revisited morphology applied for Systematic of flat wasps (Hymenoptera, Bethylinidae). Zootaxa 4752(1): 1–127. <https://doi.org/10.11646/zootaxa.4752.1.1>
- Lucena DA, Almeida EAB (2021) Morphology and Bayesian tip-dating recover deep Cretaceous-age divergences among major chrysidid lineages (Hymenoptera: Chrysididae). Zoological Journal of the Linnean Society 194(1): 36–79. <https://doi.org/10.1093/ZOOLIN-LINEAN/ZLAB010>
- Michener CD (2000) The bees of the world. John Hopkins University Press, Baltimore, 913 pp.
- Mikó I, Vilhelmsen L, Johnson NF, Masner L, Péntzes Z (2007) Skelomusculature of Scelionidae (Hymenoptera: Platygastroidea): Head and Mesosoma. Zootaxa 1571: 1–78. <https://doi.org/10.11646/zootaxa.1571.1.1>
- Móczár L (1970a) Mesitiinae of world with new genera and species. I. (Hymenoptera: Bethylinidae). Acta Zoologica Academiae Scientiarum Hungaricae 16: 175–203.
- Móczár L (1970b) New Mesitiinae from Madagascar (Hymenoptera, Bethylinidae). Annales Historico-Naturales Musel Nationalis Hungarici. Pars Zoologica 62: 317–320.
- Móczár L (1970c) Mesitiinae of world with new genera and species. II. (Hymenoptera: Bethylinidae). Acta Zoologica Academiae Scientiarum Hungaricae 16: 175–203.
- Móczár L (1970d) *Parvoculus myrmecophilus* new genus and new species from Kinshasa-Congo (Hymenoptera: Bethylinidae). Opuscula Zoologica 10: 151–153.
- Móczár L (1971a) Mesitiinae of world, genera "*Mesitius* Spinola", *Pilomesitius* Móczár, *Parvoculus* Móczár, *Pycnomesitius* Móczár e *Heterocoelia* Dahlbom. III. (Hymenoptera: Bethylinidae). Acta Zoologica Academiae Scientiarum Hungaricae 17: 295–332.
- Móczár L (1971b) *Pycnomesitius* new genus from Bethylinidae (Hymenoptera). Acta Biologica 17: 167–169.
- Móczár L (1984a) Oriental Mesitiinae (Hymenoptera, Bethylinidae). Folia Entomologica Hungarica 45: 109–150.

- Móczár L (1984b) New and little known Mesitiinae from southern Europe and Africa (Hymenoptera, Bethyridae). *Tijdschrift voor Entomologie* 127: 101113.
- Nagy CG (1969) Sur la sous-famille Mesitiinae Berland (Hym., Bethyridae). *Lucrarile Statuinea Zoologica Marina* 3: 275–300.
- Nagy CG (1972) Taxonomic remarks on Mesitiinae [sic.] (Hymenoptera, Bethyridae). *Memorie della Societa Entomologica Italiana* 51: 5–18.
- Nixon KC (1999) The parsimony Ratchet, a new method for rapid parsimony analysis. *Cladistics* 15: 407–414. <https://doi.org/10.1111/j.1096-0031.1999.tb00277.x>
- Rambaut A, Drummond AJ, Xie D, Baele G, Suchard MA (2018) Posterior summarization in Bayesian phylogenetics using Tracer 1.7. *Systematic biology* 67(5): 901–904. <https://doi.org/10.1093/sysbio/syy032>
- Ramos MS, Perkovsky EE, Rasnitsyn AP, Azevedo CO (2014) Revision of Bethyridae fossils (Hymenoptera: Bethyridae) from Baltic, Rovno and Oise amber, with comments on the Tertiary fauna of the subfamily. *Neues Jahrbuch für Geologie und Paläontologie, Abhandlungen*, 271(2): 203–228. <https://doi.org/10.1127/0077-7749/2014/0385>
- Ronchetti F, Polidori C (2020) A sting affair: A global quantitative exploration of bee, wasp and ant hosts of velvet ants. *PLoS ONE* 15(9): e0238888. <https://doi.org/10.1371/journal.pone.0238888>
- Ronquist F, Teslenko M, Van Der Mark P, Ayres DL, Darling A, Höhna S, Larget B, Liu L, Suchard MA, Huelsenbeck JP (2012) MrBayes 3.2: efficient Bayesian phylogenetic inference and model choice across a large model space. *Systematic biology* 61(3): 539–542. <https://doi.org/10.1093/sysbio/sys029>
- Rosa BB, Melo GAR, Barbeitos MS (2019) Homoplasy-based partitioning outperforms alternatives in Bayesian analysis of discrete morphological data. *Systematic biology* 68(4): 657–671. <https://doi.org/10.1093/sysbio/syz001>
- Schulmeister S (2003) Genitalia and terminal abdominal segments of male basal Hymenoptera (Insecta): morphology and Evolution. *Organisms Diversity Evolution* 3: 253–279. <https://doi.org/10.1078/1439-6092-00078>
- Sorg M (1988) Zur Phylogenie und Systematik der Bethyridae (Insecta: Hymenoptera: Chrysidoidea). *Sonderveröffentlichungen des Geologischen Institut der Universität zu Köln* 63: 1–146.
- Spinola M (1853) *Compte rendues hyménoptères inédits provenants du voyage entomologique de M. Ghilianidansle para en 1846. Memorie Reale Academia Scienze di Torino* 13: 19–94.
- Vilhelmsen L, Mikó I, Krogmann L (2010) Beyond the wasp waist: structural diversity and phylogenetic significance of the mesosoma in apocritan wasps (Insecta: Hymenoptera). *Zoological Journal of the Linnean Society* 159: 22–194. <https://doi.org/10.1111/j.1096-3642.2009.00576.x>

Appendix 1

Character list

- | | |
|--|---|
| #1. Host/
0. Lepidoptera/
1. Coleoptera/ | 0. not delimited/
1. delimited/ |
| #2. Sex dimorphism/
0. absent/
1. present/ | #10. Presence of clypeal lateral lobe/
0. absent/
1. present/ |
| #3. Length of head/
0. longer than wide/
1. as long as wide/
2. wider than long/ | #11. Shape of apex of median clypeal carina [in profile]/
0. arched/
1. straight/
2. inclined/ |
| #4. Shape of head [in profile]/
0. globoid [in lateral view]/
1. narrow [in lateral view]/ | #12. Shape of apex of median clypeal carina [in dorsal view]/
0. spoon-like shaped/
1. line shaped/ |
| #5. Layout of malar space/
0. not projected/
1. projected/ | #13. Height of median clypeal carina/
0. below torulus/
1. above torulus/ |
| #6. Length of malar space/
0. longer than VOL/
1. as long as VOL/
2. shorter than VOL/ | #14. Fusion between torulus and median carina of clypeus/
0. not fused/
1. fused/ |
| #7. Orientation of malar space/
0. convergent anteriorly/
1. parallel/ | #15. Density of pubescence of antenna/
0. sparse/
1. dense/ |
| #8. Presence of inner keel of mandible/
0. absent/
1. present/ | #16. Length of pubescence of antenna/
0. short/
1. long/
2. medium/ |
| #9. Delimitation of median lobe of clypeus/ | |

- #17. Shape of flagellomeres of antenna/
0. cylindrical shape/
1. caliciform/
- #18. Length of first flagellomere of antenna [in relation to pedicel]/
0. as long as pedicel/
1. longer than pedicel/
2. shorter than pedicel/
- #19. Length of flagellomeres 1–11 of antenna/
0. short/
1. long/
- #20. Width of flagellomeres 1–11 of antenna/
0. slender/
1. strong/
- #21. Size of eye/
0. small/
1. large/
2. very small/
- #22. Pubescence of eye/
0. absent/
1. present/
- #23. Contour of eye/
0. protruding/
1. in same level of head/
- #24. Sculpture of frons/
0. not foveolate/
1. foveolate/
- #25. Density of sculpture of frons/
0. densely foveolate/
1. sparsely foveolate/
- #26. Location of anterior ocellus of ocellar triangle/
0. placed above imaginary top line of eyes/
1. placed below imaginary top line of eyes/
2. placed at imaginary mid line of eyes/
- #27. Shape of hypostomal carina/
0. angled/
1. straight/
2. rounded/
- #28. Anterior depression of occiput/
0. absent/
1. present/
- #29. Presence of dorsal half of occipital carina/
0. absent/
1. present/
- #30. Presence of ventral half of occipital carina/
0. absent/
1. present/present, but so weakly
- #31. Shape of ventral half of postoccipital carina/
0. angled/
1. rounded/
- #32. Length of pronotal disc/
0. shorter than wide/
1. as long as wide/
2. longer than wide/
- #33. Sculpture of pronotal disc/
0. not foveolate/
1. foveolate/
- #34. Density of sculpture of pronotal disc/
0. sparse/
1. dense/
- #35. Presence of projection of corner of pronotal disc/
0. absent/
1. present/
- #36. Presence of longitudinal pronotal furrow/
0. absent or indistinct/
1. present or distinct/
- #37. Angulation anterior margin of propleuron/
0. angled/
1. straight/
2. concave/
- #38. Length of mesoscutum/
0. shorter than scutellum/
1. as long as scutellum/
2. longer than scutellum/
- #39. Presence of longitudinal furrow of mesoscutum/
0. absent/
1. present/
- #40. Presence of notaulus of mesoscutum/
0. absent/
1. present/
- #41. Orientation of notauli of mesoscutum/
0. convergent posteriorly/
1. parallel/
- #42. Impression of notaulus of mesoscutum/
0. weakly impressed/
1. well impressed/
- #43. Presence of parapsidal furrow of mesoscutum/
0. absent/
1. present/
- #44. Presence of transcupal articulation/
0. inconspicuous/
1. conspicuous/
- #45. Impression of scutoscutellar sulcus/
0. inconspicuous/
1. conspicuous/
- #46. Presence of connection between scutellar groove and axilla/
0. absent/
1. present/
- #47. Extension of scutellum/
0. not touching propodeal disc/
1. touching propodeal disc/
- #48. Length of propodeal disc/
0. shorter than half width of propodeal disc/
1. as long as half width of propodeal disc/
2. longer than half width of propodeal disc/
- #49. Metapostnotal depression/
0. absent/
1. present/
- #50. Connection between central depression and triangular lateral depression of propodeal disc/
0. absent/
1. present/
- #51. Presence of median carina of propodeal disc/
0. absent/
1. present/
- #52. Extension of median carina of propodeal disc/
0. incomplete/
1. complete/

- #53. Fusion between sublateral and inner discal carina of propodeal disc/
0. absent/
1. present/
- #54. Presence of inner discal carina of propodeal disc/
0. absent/
1. present/
- #55. Extension of inner discal carina of propodeal disc/
0. incomplete/
1. complete/
- #56. Orientation of inner discal carina of propodeal disc/
0. parallel with median carina/
1. not parallel with median carina/
- #57. Presence of sublateral carina of propodeal disc/
0. absent/
1. present/
- #58. Presence of lateral carina of propodeal disc/
0. absent/
1. present/
- #59. Presence of posterior carina of propodeal disc/
0. absent/
1. present/
- #60. Extension of posterior carina of propodeal disc/
0. incomplete medially/
1. complete/
- #61. Shape of propodeal spiracle/
0. elliptical/
1. circular/
- #62. Location of propodeal spiracle/
0. placed at dorsal surface of propodeum/
1. placed at lateral surface of propodeum/
- #63. Presence of posterior spine of propodeum/
0. absent/
1. present/
- #64. Width of posterior spine of propodeum/
0. thick/
1. slender/
- #65. Presence of median carina of declivity of propodeum/
0. absent/
1. present/
- #66. Presence of lateral carina of declivity of propodeum/
0. absent/
1. present/
- #67. Presence of superior carina of side of propodeum/
0. absent/
1. present/
- #68. Mesopleuron foveae distinction/
0. absent/
1. present/
- #69. Presence of posterior carina of side of propodeum/
0. absent/
1. present/
- #70. Fusion between subtegular fovea and episternal furrow of mesopleuron/
0. not fused/
1. fused/
- #71. Presence of transverse furrow of mesopleuron/
0. absent/
1. present/
- #72. Presence of diastema between tegula and mesoscutum/
0. absent/
1. present/
- #73. Presence of costal vein of forewing/
0. absent/
1. present/
- #74. Shape of transverse median vein of forewing/
0. bi-angulate/
1. rounded/
- #75. Presence of nebulous cubital vein of forewing/
0. absent/
1. present/
- #76. Presence of nebulous anal vein of forewing/
0. absent/
1. present/
- #77. Presence of distal fusion among costal and subcostal vein before stigma of forewing/
0. absent/
1. present/
- #78. Presence of proximal hamuli of hind wing/
0. absent/
1. present/
- #79. Number of proximal hamuli of hind wing/
0. one/
1. two/
2. three/
3. six/
- #80. Presence of distal hamuli of hind wing/
0. absent/
1. present/
- #81. Number of distal hamuli of hind wing/
0. three/
1. four/
2. one/
3. five/
- #82. Distance between distal hamuli of hind wing/
0. separated each other by uniform space/
1. first hamuli more separated than others/
- #83. Presence of dorsal process of hind coxa/
0. absent/
1. present/
- #84. Shape of tarsal claw/
0. one tooth/
1. two teeth/
2. three teeth/
- #85. Presence of constriction between tergum I and tergum II of metasoma/
0. absent/
1. present/
- #86. Presence of ventral sculpture at tergum I of metasoma/
0. absent/
1. present/
- #87. Presence of lateral ventral lap of tergum I of metasoma/
0. absent/
1. present/
- #88. Presence of dorsal setae at tergum I of metasoma/

0. absent/
1. present/
#89. Length of tergum II of metasoma/
0. as long as others/
1. longer than others/
#90. Type of dorsal texture of tergum II of metasoma/
0. polished/
1. coriaceous/
#91. Presence of dorsal sculpture of tergum II of metasoma/
0. absent/
1. present/
#92. Presence of ventral sculpture of tergum II of metasoma/
0. absent/
1. present/
#93. Type of ventral texture of tergum II of metasoma/
0. polished/
1. coriaceous/
#94. Length of hypopygium/
0. longer than wide/
1. as long as wide/
2. wider than long/
#95. Width of median anterior process of hypopygium/
0. acute/
1. wide/
#96. Shape of posterior margin of hypopygium/
0. simple/
1. bilobed
#97. Shape of branches of posterior margin of hypopygium/
0. lobose/
1. filamentary/
#98. Length of branches of posterior margin of hypopygium/
0. short/
1. long/
#99. Orientation of lateral margin of hypopygium/
0. parallel/
1. convergent/
#100. Presence of lateral anterior projection of hypopygium/
0. absent/
1. present/
#101. Presence of projection of genital ring/
0. absent/
1. present/
#102. Number of paramere arms of genitalia/
0. one/
1. two/
#103. Shape of dorsal arm of paramere of genitalia/
0. “S” shaped/
1. club-shaped/
2. filamentary shaped/
#104. Shape of ventral arm of paramere of genitalia/
0. club-shaped/
1. “S” shaped/
#105. Presence of fusion between basiparamere and basivolsella of genitalia/
0. absent/
1. present/
#106. Number of arms of cuspis of genitalia/
0. one/
1. two/
#107. Arms of cuspis of genitalia/
0. distinct/
1. hardly distinct/
#108. Width of aedeagus of genitalia/
0. slender/
1. wide/
#109. Length of aedeagus of genitalia/
0. not reaching paramere apex/
1. surpassing paramere apex/
2. aligned with paramere apex/
#110. Apex shape of aedeagus of genitalia/
0. rounded/
1. truncate/
2. angled/
#111. Presence of apical sickle process of aedeagus of genitalia/
0. absent/
1. present/
#112. Shape of lateral margin of aedeagus basal portion of genitalia/
0. convex/
1. straight/

Supplementary material 1

Table S1

Authors: Barbosa DN, Hermes MG, Lepeco A (2022)

Data type: .xlsx

Explanation note: Matrix of coded state characters related to each taxon.

Copyright notice: This dataset is made available under the Open Database License (<http://opendatacommons.org/licenses/odbl/1.0>). The Open Database License (ODbL) is a license agreement intended to allow users to freely share, modify, and use this Dataset while maintaining this same freedom for others, provided that the original source and author(s) are credited.

Link: <https://doi.org/10.3897/asp.80.e86666.suppl1>

Supplementary material 2

Table S2

Authors: Barbosa DN, Hermes MG, Lepeco A (2022)

Data type: .xlsx

Explanation note: Mesitiinae genera, their number of species and type species of in its original combination.

Copyright notice: This dataset is made available under the Open Database License (<http://opendatacommons.org/licenses/odbl/1.0>). The Open Database License (ODbL) is a license agreement intended to allow users to freely share, modify, and use this Dataset while maintaining this same freedom for others, provided that the original source and author(s) are credited.

Link: <https://doi.org/10.3897/asp.80.e86666.suppl2>

Supplementary material 3

Figure S1

Authors: Barbosa DN, Hermes MG, Lepeco A (2022)

Data type: .pdf

Explanation note: Symmetric resampling of cladistic analysis tree.

Copyright notice: This dataset is made available under the Open Database License (<http://opendatacommons.org/licenses/odbl/1.0>). The Open Database License (ODbL) is a license agreement intended to allow users to freely share, modify, and use this Dataset while maintaining this same freedom for others, provided that the original source and author(s) are credited.

Link: <https://doi.org/10.3897/asp.80.e86666.suppl3>

Supplementary material 4

Figure S2

Authors: Barbosa DN, Hermes MG, Lepeco A (2022)

Data type: .pdf

Explanation note: Bayesian tree based on partitioned parameters, indicating posterior probability for each node.

Copyright notice: This dataset is made available under the Open Database License (<http://opendatacommons.org/licenses/odbl/1.0>). The Open Database License (ODbL) is a license agreement intended to allow users to freely share, modify, and use this Dataset while maintaining this same freedom for others, provided that the original source and author(s) are credited.

Link: <https://doi.org/10.3897/asp.80.e86666.suppl4>

Supplementary material 5

Figure S3

Authors: Barbosa DN, Hermes MG, Lepeco A (2022)

Data type: .pdf

Explanation note: Bayesian tree based on unpartitioned parameters, indicating posterior probability for each node.

Copyright notice: This dataset is made available under the Open Database License (<http://opendatacommons.org/licenses/odbl/1.0>). The Open Database License (ODbL) is a license agreement intended to allow users to freely share, modify, and use this Dataset while maintaining this same freedom for others, provided that the original source and author(s) are credited.

Link: <https://doi.org/10.3897/asp.80.e86666.suppl5>